1-1-1993

Crystal-Field Symmetry And Ordered Phases In Arrays Of Helical Xy Spin Chains

O. Heinonen
University of Central Florida

Crystal-field symmetry and ordered phases in arrays of helical XY spin chains

O. Heinonen
Department of Physics, University of Central Florida, Orlando, Florida 32816
(Received 21 April 1992; revised manuscript received 21 July 1992)

The effect of crystal-field symmetry and strength on the nature of ordered phases in three-dimensional systems consisting of arrays of helical XY spin chains is investigated. The phase diagrams of chiral chains in arrays with twofold symmetry always exhibit a Lifshitz point, where paramagnetic, ferromagnetic, and incommensurate phases meet. In contrast, the phase diagrams of chains in arrays in which the crystal field has higher symmetry than twofold have no Lifshitz point, whether the chains are chiral or not. In these arrays, the initial phase transition is always paramagnetic to incommensurate. The existence of a Lifshitz point in the phase diagram of nonchiral chains in arrays with twofold symmetry depends sensitively on the interchain coupling.

I. INTRODUCTION

A variety of physical systems, such as magnetic systems, binary alloys, and lipid bilayers, exhibit spatially modulated phases. These spatial modulations arise from competing interactions. Some systems with competing interactions have been modeled by, for example, the anisotropic next-nearest-neighbor Ising model (ANNNI),[1–3] and the chiral-clock model.[2,4] The phase diagrams of these models in three dimensions are in general very complex, but are well described by mean-field theories[5,6] and have the following qualitative features. Let κ be a parameter denoting the relative strength of the competing interactions. The phase diagram in the $(T-\kappa)$ plane can in general be divided into two parts. In one, the disorder-order phase transition is paramagnetic to ferromagnetic. In the other part of the phase diagram, on the other hand, the transition is from a paramagnetic phase to incommensurate one, with many subsequent modulated phases as the temperature is further reduced. The paramagnetic, ferromagnetic, and incommensurate phases all meet at the Lifshitz point.

Competing interactions also arise in many crystalline polymers. In these systems, isolated chains have helical conformations with a pitch incommensurate with the monomer spacing along the chain, i.e., the displacement of torsional angle between successive monomers is not a simple rational fraction of 2π. The reason for this is that the pitch is determined by a complicated sum of interatomic forces. Unless the molecule itself has some particular symmetry, the pitch resulting from this sum is incommensurate with the monomer spacing. When the polymer molecules are packed in a regular array, however, the interchain interactions typically favor a commensurate ordering. The conformations of the molecules are then determined by the interplay between the competing intrachain and interchain interactions, as well as the temperature and external field. It has been shown that at absolute zero of temperature, the polymer molecules in a regular array form a commensurate structure.[7,8] As the temperature is increased, the entropic contribution to the free energy increases, and commensurate structures other than the one which minimizes the internal energy, as well as incommensurate structures, may become energetically favorable. At elevated temperatures, there are polymer systems which have been observed to display phases with both commensurate and incommensurate structures. It has also been observed experimentally that the individual molecules in some crystalline polymers become disordered as the temperature is increased but remains below the melting temperature of the lattice of chains. One example is the polymer polytetrafluoroethylene (PTFE).[9] The phase diagram of this polymer is displayed in Fig. 1. In the high-temperature phases I and IV, the polymer chains form commensurate helices, and in phase I they have a large amount of helical disorder.[10] In the low-temperature phase II, the chains are ordered incommensurate helices.[11] In these three phases, the packing of the chains is hexagonal. In the high-pressure phase III, on the other hand, the unit cell is orthorhombic and the

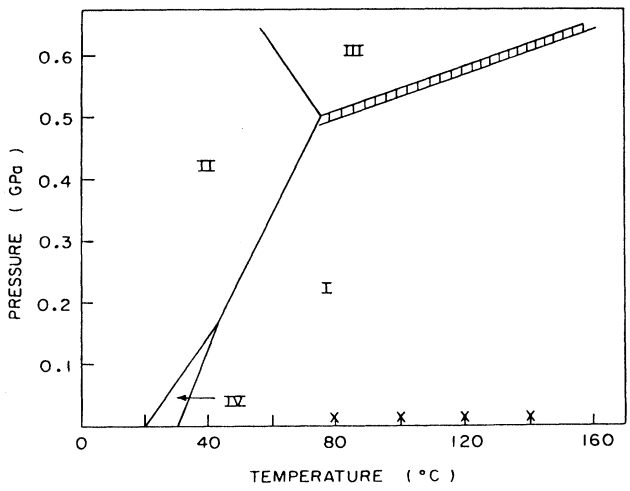

FIG. 1. Phase diagram in the PT plane of PTFE.

molecules have planar zigzag conformations.

In many cases, the physical properties of a polymer system depend on the helical conformation of the molecules. It is therefore important to understand how this conformation is affected by intrachain and interchain interactions and temperature, as well as external fields. The motivation for the work presented here was to qualitatively describe the phase diagram of such systems. Most helical polymer molecules are degenerate in the sense that an isolated chain is equally likely to be a right-handed helix or a left-handed helix. However, there exist whole classes of polymers which have a preferred chirality. We shall refer to such systems as chiral systems, in contrast to systems with no preferred handedness, which we shall call nonchiral. Important examples of chiral molecules are biomolecules such as nucleic acids and α-amino proteins.[12,13] Recent developments in the synthesis of polymers have also led to heliospecific polymerization in which chiral polymers are synthesized with a specific handedness. Therefore, it is important to understand how chirality may affect the phase diagram of these systems. We have investigated how the symmetry and strength of the crystal field (the precise meaning of the crystal field will be given later) affect the nature of the phase diagram of three-dimensional systems consisting of arrays of helical XY spin systems, both chiral and nonchiral. Preliminary results on the initial order-disorder transition for chiral systems in the limit of very large crystal-field strength, appropriate for polymers, were published earlier.[14] In the present paper, we present a more complete and general account of both chiral and nonchiral systems. Our main result is that for chiral helices in crystal fields with twofold symmetry, for example, arrays with an orthorhombic structure, the disorder-order transition dramatically changes character as a function of crystal-field strength. The transition changes from a high-temperature paramagnetic-incommensurate phase transition to a paramagnetic-ferromagnetic phase transition. This crossover occurs for all values of the preferred pitch of an isolated helix (although the exact location in the phase diagram of the crossover depends on this pitch). The crossover implies the existence of a Lifshitz point in the phase diagram. If the crystal field has higher symmetry than twofold, on the other hand, the order-disorder transition occurs (almost) always[15] to an initial incommensurate phase and there is no Lifshitz point, whether the chains are chiral or not. As the temperature is further reduced, the system exhibits a sequence of modulated phases. Finally, nonchiral systems in arrays with twofold may exhibit Lifshitz points only if the interchain interactions are weak.

This paper is organized as follows. In Sec. II we will discuss the general form of the Hamiltonians that we will consider, and in Sec. II A chiral models are studied. In Sec. II B we will discuss nonchiral models, and Sec. III contains a discussion and conclusions.

II. GENERAL MODEL

We are considering systems which can be described as an array of chains of M classical XY spins equidistantly spaced with a separation d along the z axis. Polymer molecules, for example, can be thought of as a set of directed monomers pointing in the xy plane, and the spins represent the angles which the directed monomers make with respect to the x axis. The spins are free to rotate in the xy plane and are positioned at $\mathbf{r}_{i,j}$, where the index i denotes the position along the z axis, and j is an index denoting the chain. We will assume that $\mathbf{r}_{i,j}$ forms a regular lattice with the property that $\hat{\mathbf{z}}\cdot\mathbf{r}_{i,j}=\hat{\mathbf{z}}\cdot\mathbf{r}_{i,j'}$. The spin at $\mathbf{r}_{i,j}$ is denoted $\mathbf{S}_{i,j}=\cos\theta_{i,j}\hat{\mathbf{x}}+\sin\theta_{i,j}\hat{\mathbf{y}}$, where $\theta_{i,j}$ is the angle between $\mathbf{S}_{i,j}$ and the x axis. We write the Hamiltonian as a sum of intrachain and interchain terms, $H=H_0+H_{\text{inter}}$. The specific form of the intrachain part H_0 will depend on if the model is chiral or nonchiral. We will restrict the interchain part H_{inter} to include only nearest-neighbor interactions. In addition to the nearest-neighbor spin-spin interactions, we expect that this part will contain a term describing the interaction of a monomer with its average crystalline environment. This term will explicitly contain the symmetry of the lattice of chains. We identify these two components of H_{inter} by first writing the potential energy of in-plane nearest-neighbor interactions as a sum of pair potentials, and expand the monomer mass densities in multipoles.[14] To first order we obtain a term proportional to $\cos(\theta_{i,j}-\theta_{i,j'})$. Averaging over the angles and summing over nearest neighbors removes the angular dependence of all terms up to nth order, where n is the symmetry of the chain packing, i.e., $n=6$ for hexagonal packing and $n=4$ for a square lattice. To nth order, we find a term proportional to $\cos(n\theta_{i,j})$. This is the term that has the symmetry of the lattice. The Hamiltonian is then

$$H=NH_0+\gamma\sum_{i,j}\cos(n\theta_{i,j})-\tfrac{1}{2}J_\perp\sum_{\substack{i\\ \langle j,j'\rangle}}\cos(\theta_{i,j}-\theta_{i,j'}). \tag{2.1}$$

Here N is the number of chains, and $\langle j,j'\rangle$ means that the summation extends over nearest-neighbor chains j and j'. The parameter γ is a measure of what we shall here call the crystal-field strength. Note that both the value of γ as well as the symmetry of the crystal field can be affected by the application of, for example, isotropic pressure and uniaxial stress, as well as other external fields.

We separate the Hamiltonian equation (2.1) into an effective single-chain piece,

$$H_1=H_0+\gamma\sum_i\cos(n\theta_{i,j}), \tag{2.2}$$

and an interchain piece

$$H_2=-\tfrac{1}{2}J_\perp\sum_{\substack{\langle j,j'\rangle\\ i}}\cos(\theta_{i,j}-\theta_{i,j'}). \tag{2.3}$$

In addition, we will sometimes couple an external field $\mathbf{F}(\mathbf{r}_{i,j})$ conjugate to the spin variables to the Hamiltonian defined by equation (2.1), which adds a term $-\sum_{i,j}\mathbf{F}(\mathbf{r}_{i,j})\cdot\mathbf{S}(\mathbf{r}_{i,j})$. This field need not be a physically

realizable field, but is a convenient device for considering an initial phase transition from a disordered (paramagnetic) phase to an ordered one.

The strategy that we will adopt is to treat the single-chain Hamiltonian equation (2.2) as exactly as possible, and then to add approximations for the interchain interactions. This is a reasonable approximation for pseudo-one-dimensional systems in which the intrachain correlations are much stronger than the interchain correlations, and has been applied successfully to polymers and other systems in earlier work.[3,16,17] We also note that mean-field approximations (both in-plane and along the axes) applied to, for example, the ANNNI model gives excellent results concerning the structure of the ordered phases for three-dimensional systems. Therefore, we believe that the effects addressed here can be well described by the approximations that we shall use.[18]

Our focus will be on how the crystal field and temperature affect the chain conformations in the ordered phases. These conformations will be studied through the intrachain susceptibilities

$$\chi^{\mu\nu}(\mathbf{r}_{i,j},\mathbf{r}_{i',j'}) = \beta\langle S_\mu(\mathbf{r}_{i,j})S_\nu(\mathbf{r}_{i',j'})\rangle - \beta\langle S_\mu(\mathbf{r}_{i,j})\rangle\langle S_\nu(\mathbf{r}_{i',j'})\rangle, \quad \mu,\nu = x,y, \tag{2.4}$$

where $\beta = 1/(k_BT)$ and angular brackets denote thermal averages. In particular, if the Fourier transform of $\chi^{\mu\nu}$ has a maximum at a wave vector with a finite component q_z, then the chains have a helical conformation with an average pitch $q_z d$.

A. Chiral models

We first consider chiral models. As we mentioned in the Introduction, there are many important physical systems that are chiral. In addition, chiral Hamiltonians with only nearest-neighbor intrachain interactions exhibit modulated phases, whereas nonchiral models require at least nearest-neighbor and next-nearest-neighbor interactions to exhibit modulated phases, which leads to considerably more complicated models.

As a model intrachain Hamiltonian H_0, we take

$$H_0 = -J_\parallel \sum_i \cos(\theta_{i,j} - \theta_{i-1} - \alpha), \tag{2.5}$$

$J_\parallel > 0$. The ground state of the Hamiltonian H_0 is then a right-handed helix with pitch α. This pitch is determined only by intrachain interactions and is in general not a rational fraction of 2π. We start by investigating the effective single-chain Hamiltonian

$$H_1 = -J_\parallel \sum_i \cos(\theta_i - \theta_{i-1} - \alpha) + \gamma \sum_i \cos(n\theta_{i-1}), \tag{2.6}$$

where we have dropped the chain subscript j. We note that we can restrict α to $\alpha \in [0, \pi/n)$. For α larger than π/n we make the substitutions by $\theta_i \rightarrow \theta_i + i2\pi m/n$ $(i = 1,2,\ldots,M)$ and $\alpha \rightarrow \alpha - 2\pi m/n$, where m is the smallest integer such that $2\pi m/n - \alpha > 0$ and $m \leq n$. This has as a consequence that commensurate order with a pitch $2\pi m/n$ $(0 \leq m \leq n)$ and ferromagnetic orders are equivalent within our formalism.

The properties of the Hamiltonian equation (2.6) are most easily studied within a transfer-integral formalism.[19] The transfer-integral equation for a single chain is

$$\int_{-\pi}^{\pi} \frac{d\theta_i}{2\pi} e^{\beta J_\parallel \cos(\theta_i - \theta_{i-1} - \alpha) - \beta\gamma\cos(n\theta_{i-1})} \Psi_k(\theta_i) = \lambda_k \Psi_k(\theta_{i-1}). \tag{2.7}$$

Here $\Psi_k(\theta)$ and λ_k are the right eigenfunctions and the corresponding eigenvalues of the transfer-integral operator. The integral kernel in Eq. (2.7) is not symmetric for $\alpha \neq 0$. Hence, the left and right eigenfunctions are in general not equal, and the eigenvalues are in general complex. However, the largest eigenvalue, λ_0, is always real since the integral kernel is real. It is easy to show that the left eigenfunctions $\Phi_k(\theta)$ are related to $\Psi_k(\theta)$ by

$$\Phi_k(\theta) = \Psi_k(-\theta)e^{\beta\gamma\cos(n\theta)}. \tag{2.8}$$

With the appropriate normalization of the eigenfunctions Φ_k and Ψ_k, the correlation function can be expressed in terms of these eigenfunctions as

$$\langle S_\mu(\theta_i)S_\nu(\theta_{i'})\rangle = \sum_k \langle\Phi_0|S_\mu(\theta_i)|\Psi_k\rangle\langle\Phi_k|S_\nu(\theta_{i'})|\Psi_0\rangle \left(\frac{\lambda_k}{\lambda_0}\right)^{|i-i'|}, \tag{2.9}$$

where

$$\langle\Phi_k|f|\Psi_{k'}\rangle = \int_{-\pi}^{\pi} d\theta \Phi_k(\theta)\Psi_{k'}(\theta)f(\theta). \tag{2.10}$$

The n-fold symmetry of the crystal-field term causes the solutions of Eq. (2.7) to be in the form of Bloch functions, namely

$$\Psi_k(\theta) = \exp(ip\theta)\, u_k(\theta) \tag{2.11}$$

with p an integer and $u_k(\theta)$ a periodic function of period $2\pi/n$ (we use roman i to denote the imaginary unit, and italic i to denote a site index). The eigenvalues λ_k, which are in general complex, then occur in bands, and can be written as $\lambda_{m,p}$ with m a non-negative integer representing the band index and p an integer with $-n/2 < p \leq n/2$. The matrix elements appearing in Eq. (2.9) are then of the form

$$\int_{-\pi}^{\pi} d\theta \Phi_{m,p}(\theta)\Psi_{m',p'}(\theta)f(\theta), \tag{2.12}$$

with $f(\theta) = \cos\theta$ or $\sin\theta$, and these will vanish unless $p' = p \pm 1$. (In the case $n = 2$, there are only two eigenvalues in the band $m = 0$. If the second largest eigenvalue is complex, we let $\lambda_{0,\pm1}$ denote this eigenvalue

and its complex conjugate.) Equation (2.9) then reduces to

$$\langle S_\mu(\theta_i)S_\nu(\theta_{i'})\rangle = \sum_m \langle\Phi_{0,0}|S_\mu(\theta_i)|\Psi_{m,\pm1}\rangle\langle\Phi_{m,\pm1}|S_\nu(\theta_{i'})|\Psi_{0,0}\rangle\left[\frac{\lambda_{m,\pm1}}{\lambda_{0,0}}\right]^{|i-i'|}. \tag{2.13}$$

The correlations will be dominated by the closest excited states coupled by $S_\mu(\theta_i)$ to the ground state $\Psi_{0,0}$. Hence, we retain only the term with $m = 0$ in Eq. (2.13). By defining

$$\begin{aligned}
&\langle\Phi_{0,0} \mid \cos\theta \mid \Psi_{0,1}\rangle \equiv a_x,\\
&\langle\Phi_{0,0} \mid \sin\theta \mid \Psi_{0,1}\rangle \equiv a_y,\\
&\langle\Phi_{0,1} \mid \cos\theta \mid \Psi_{0,0}\rangle \equiv b_x = a_x,\\
&\langle\Phi_{0,1} \mid \sin\theta \mid \Psi_{0,0}\rangle \equiv b_y = -a_y,
\end{aligned} \tag{2.14}$$

where $a_y = \mathrm{i}(1-a_x)$, and using the relationship between the right and left eigenfunctions given Eq. (2.8) together with the fact that eigenfunctions belonging to complex conjugate eigenvalues are themselves complex conjugate, $\Psi_{m,-p} = \Psi^*_{m,p}$ if $\lambda_{m,-p} = \lambda^*_{m,p}$, we arrive at the following result for the single-chain susceptibilities $\chi_0^{\mu\nu}$:

$$\begin{aligned}
\chi_0^{xx}(i-i') &= 2\beta\Gamma^{-|i-i'|}\Re\left[a_x^2 e^{-\mathrm{i}\phi|i-i'|}\right],\\
\chi_0^{yy}(i-i') &= -2\beta\Gamma^{-|i-i'|}\Re\left[a_y^2 e^{-\mathrm{i}\phi|i-i'|}\right],\\
\chi_0^{xy}(i-i') &= -\chi_0^{yx}(i-i')\\
&= -2\beta\Gamma^{-|i-i'|}\Re\left[a_x a_y e^{-\mathrm{i}\phi|i-i'|}\right].
\end{aligned} \tag{2.15}$$

Here, $\lambda_{0,1}/\lambda_{0,-1} \equiv \Gamma e^{\mathrm{i}\phi}$, and $\Re$ denotes the real part. In the case that $\lambda_{0,1}$ is real and positive, the correlation functions are exponentially decaying. Hence, the Fourier transform has a maximum at $q_z = 0$ and the intrachain correlations are ferromagnetic. In the case that $\lambda_{0,1}$ is real and negative, we can write

$$\chi_0^{\mu\nu}(i-i') = 2\beta\Gamma^{-|i-i'|}\Re\left[a_\mu b_\nu e^{\mathrm{i}\pi|i-i'|}\right]. \tag{2.16}$$

Fourier transforming then yields antiferromagnetic intrachain correlations. This case has been eliminated by a suitable redefinition of α and θ_i as discussed earlier. If $\lambda_{0,1}$ is complex, then $\lambda_{0,-1} = \lambda^*_{0,1}$. The Fourier transform then becomes

$$\chi_0^{\mu\nu}(q_z) = 2\frac{\Re(a_\mu b_\nu) - \Gamma\Re\left[a_\mu b_\nu e^{\mathrm{i}\phi+\mathrm{i}q_z d}\right]}{1+\Gamma^2-2\Gamma\cos(q_z d+\phi)} + 2\frac{\Re(a^*_\mu b\nu^*) - \Gamma\Re\left[a^*_\mu b^*_\nu e^{-\mathrm{i}\phi+\mathrm{i}q_z d}\right]}{1+\Gamma^2-2\Gamma\cos(q_z d-\phi)} + 2\Re(a_\mu b_\nu).$$

This shows that the correlations are dominated by the Fourier components $q_z d = \pm\phi$. Thus, the argument of $\lambda_{0,1}$ always determines the conformation of the isolated chain. We shall find that when interchain interactions are added, the intrachain correlations are dominated by their values for an isolated chain, and the nature of the ordered phases depends strongly on these correlations. (Note that we will here only consider ferromagnetic interchain correlations which do not further frustrate the system.)

We can easily solve for the eigenvalues and eigenfunctions of the transfer-integral equation (2.7) in the limits $\beta\gamma \to 0$ and $\beta\gamma \to \infty$, while $\gamma/J_\parallel$ remains finite and nonzero. In the limit $\beta\gamma \to 0$, the eigenfunctions are

$$\Psi_{\pm k}(\theta) = e^{\pm\mathrm{i}k\theta}, \tag{2.17}$$

and the corresponding eigenvalues are

$$\lambda_{\pm k} = e^{\pm\mathrm{i}k\alpha} I_k(\beta J_\parallel), \tag{2.18}$$

where $I_k(x)$ is a modified Bessel function of order k. It is then straightforward to obtain $a_x = 1/2$ and $a_y = i/2$, so that

$$\begin{aligned}
\chi_0^{xx}(i) &= \frac{\beta}{2}\cos(i\alpha)\frac{I_1(\beta J_\parallel)}{I_0(\beta J_\parallel)},\\
\chi_0^{xy}(i) &= \frac{\beta}{2}\sin(i\alpha)\frac{I_1(\beta J_\parallel)}{I_0(\beta J_\parallel)}.
\end{aligned} \tag{2.19}$$

In the limit $\beta\gamma \to \infty$, in which the model becomes equivalent with the p-state chiral-clock model, we expand $\exp[-\beta\gamma\cos(n\theta_{i-1})]$ to second order about $\theta_{i-1} = (2p+1)\pi/n$ to obtain

$$e^{-\beta\gamma\cos(\theta_{i-1})} \approx \frac{e^{\beta\gamma}}{\sqrt{2\pi n^2\beta\gamma}}\sum_{p=0}^{n-1}\delta[\theta_{i-1}-(2p+1)\pi/n]. \tag{2.20}$$

The eigenvalue problem then separates into an $n\times n$ matrix for each Bloch band. Hence, for $n = 2$ the two largest eigenvalues are always real, whereas for $n > 2$, the second largest eigenvalue is in general complex. We then conclude that in this limit, the intrachain correlations are always ferromagnetic for $n = 2$, whereas they are helical ($\phi \neq 0$) for $n > 2$.[20]

The question then arises how the phase ϕ of $\lambda_{0,1}$, and hence the intrachain correlations, depends on $\beta\gamma$. In particular, the above limiting cases show that for $n = 2$ there

must be a transition from $\lambda_{0,1}$ complex to real as $\beta\gamma$ increases. In Fig. 2 we have plotted the argument of $\lambda_{0,1}$ for various values of γ as a function of temperature for $n = 2$ and $n = 3$. We note that for $n = 3$, the arguments go smoothly from zero as $\beta \to \infty$ to α as $\beta \to 0$. For $n = 2$, on the other hand, the arguments become zero at $\beta\gamma \sim 1$.

We now add interchain spin-spin interactions given by the Hamiltonian H_2 in Eq. (2.3), and turn to the conformations of ordered phases. The behavior of the spin-spin correlations of the isolated chain leads us to the following conjecture. For $n > 2$, the initial phase transition from a high-temperature disordered phase will (almost) always occur to an incommensurate phase because the single chain is helical with a pitch which depends smoothly on temperature. Hence, the phase diagrams of these systems contain no Lifshitz point. For $n = 2$, however, the isolated chain becomes ferromagnetic if $\beta\gamma$ is larger than some critical value $(\beta\gamma)_{\rm cr}$. If, when interchain interactions are added, the order-disorder transition occurs at a temperature low enough that $\beta\gamma > (\beta\gamma)_{\rm cr}$, the intrachain correlation will already have developed ferromagnetic order. Hence, such a phase transition must occur directly to a ferromagnetic phase. This implies the existence of a Lifshitz point for $\gamma = \gamma_{\rm cr}$.

We test this conjecture by a method due to Scalapino, Imry, and Pincus.[21] We add an external field conjugate to the spins. The total Hamiltonian is thus

$$H = -J_{\parallel}\sum_{ij}\cos\left(\theta_{i,j} - \theta_{i-1,j} - \alpha\right) - \frac{1}{2}J_{\perp}\sum_{\substack{i\\ \langle jj'\rangle}}\left[\cos\theta_{ij}\cos\theta_{ij'} + \sin\theta_{ij}\sin\theta_{ij'}\right] + \gamma\sum_{ij}\cos(n\theta_{ij}) - \sum_{ij}\mathbf{F}(\mathbf{r}_{ij})\cdot\mathbf{S}(\mathbf{r}_{ij}). \tag{2.21}$$

The susceptibility can, by the fluctuation–dissipation theorem, be related to the linear response of $\langle S_\mu(\mathbf{r}_{ij})\rangle$ to an applied field $\mathbf{F}(\mathbf{r}_{ij})$. We treat the chains as pseudo one dimensional and calculate the susceptibility $\chi^{\mu\nu}(\mathbf{q})$ in a scheme where the interchain couplings are treated in the mean-field approximation. In this approximation, the Hamiltonian is then written

$$H_{\rm mf} = -J_{\parallel}\sum_{ij}\cos(\theta_{i,j} - \theta_{i-1,j} - \alpha) - \frac{1}{2}J_{\perp}\sum_{\substack{i\\ \langle jj'\rangle}}\left[\cos\theta_{ij}\langle\cos\theta_{ij'}\rangle + \sin\theta_{ij}\langle\sin\theta_{ij'}\rangle\right] + \gamma\sum_{ij}\cos(n\theta_{ij}) - \sum_{ij}\mathbf{F}(\mathbf{r}_{ij})\cdot\mathbf{S}(\mathbf{r}_{ij}). \tag{2.22}$$

Upon introducing the Fourier transform of the mean fields,

$$S_x(\mathbf{q}) = \frac{1}{N}\sum_{ij'}\langle\cos\theta_{ij'}\rangle e^{-i\mathbf{q}\cdot\mathbf{r}_{ij'}}, \tag{2.23}$$

$$S_y(\mathbf{q}) = \frac{1}{N}\sum_{ij'}\langle\sin\theta_{ij'}\rangle e^{-i\mathbf{q}\cdot\mathbf{r}_{ij'}}, \tag{2.24}$$

and of the applied field

$$\mathbf{F}(\mathbf{q}) = \frac{1}{N}\sum_{ij}\mathbf{F}(\mathbf{r}_{ij})e^{-i\mathbf{q}\cdot\mathbf{r}_{ij}}, \tag{2.25}$$

the mean-field Hamiltonian becomes

$$H_{\rm mf} = -J_{\parallel}\sum_{ij}\cos(\theta_{ij} - \theta_{i-1,j} - \alpha) + \gamma\sum_{ij}\cos(n\theta_{ij}) - \frac{1}{2}\sum_{\mathbf{q},ij}J_{\perp}(q_{\perp})e^{i\mathbf{q}\cdot\mathbf{r}_{ij}}\mathbf{S}(\mathbf{r}_{ij})\cdot\mathbf{S}(\mathbf{q}) - \sum_{\mathbf{q},ij}\mathbf{F}(\mathbf{q})\cdot\mathbf{S}(\mathbf{r}_{ij})e^{i\mathbf{q}\cdot\mathbf{r}_{ij}} \tag{2.26}$$

where

$$J_{\perp}(q_{\perp}) = J_{\perp}(q_x, q_y) = J_{\perp}\sum_{j'}e^{i\mathbf{q}\cdot(\mathbf{r}_{ij'} - \mathbf{r}_{ij})}, \tag{2.27}$$

with j' nearest neighbors to j. This shows that $\mathbf{S}(\mathbf{r}_{ij})$ is subjected to an effective external field $\mathbf{h}(\mathbf{r}_{ij})$ given by

$$\mathbf{h}(\mathbf{r}_{ij}) = \sum_{\mathbf{q}}\mathbf{h}(\mathbf{q})e^{i\mathbf{q}\cdot\mathbf{r}_{ij}} = \sum_{\mathbf{q}}e^{i\mathbf{q}\cdot\mathbf{r}_{ij}}\left[\mathbf{F}(\mathbf{q}) - J_{\perp}(q_{\perp})\mathbf{S}(\mathbf{q})\right]. \tag{2.28}$$

For a single chain, $S_x(q_z)$ and $S_y(q_z)$ are related to the external field by the single-chain susceptibility $\chi_0^{\mu\nu}(q_z)$, so that

$$S_\mu(q_z) = \sum_{\nu}\chi_0^{\mu\nu}(q_z)h_\nu(q_z). \tag{2.29}$$

Thus, by combining Eqs. (2.28) and (2.29) we obtain for the array of chains

$$\sum_{\nu}S_\nu(\mathbf{q})\left[\delta_{\mu\nu} - J_{\perp}(q_{\perp})\chi_0^{\mu\nu}(q_z)\right] = \sum_{\nu}F_\nu(\mathbf{q})\chi_0^{\mu\nu}(q_z). \tag{2.30}$$

The susceptibilities $\chi^{\mu\nu}(\mathbf{q})$ are then related to those of a single chain, $\chi_0^{\mu\nu}(q_z)$, by

$$\chi^{\mu\nu}(\mathbf{q}) = \sum_{\mu'} \left\{ [1 - J_\perp(q_\perp)\chi_0(q_z)]^{-1} \right\}_{\mu\mu'} \chi_0^{\mu'\nu}(q_z). \tag{2.31}$$

At certain temperatures and wave vectors, we will find that the matrix $[1 - J_\perp(q_\perp)\chi_0(q_z)]$ becomes singular, which we will interpret as a spontaneous ordering of the chains into the structures given by these wave vectors. This leads to the determinantal equation

$$\begin{vmatrix} J_\perp(q_\perp)\chi_0^{xx}(q_z) - 1 & J_\perp(q_\perp)\chi_0^{xy}(q_z) \\ J_\perp(q_\perp)\chi_0^{yx}(q_z) & J_\perp(q_\perp)\chi_0^{yy}(q_z) - 1 \end{vmatrix} = 0. \tag{2.32}$$

The largest temperature at which solutions to this equation exist is then the physically relevant transition temperature.

If we insert the results from above in the limits $\gamma \to 0$ and $\gamma \to \infty$ for $\chi_0^{\mu\nu}(q_z)$, the equation determining the phase transition becomes

$$\frac{1 - \Gamma^2}{1 + \Gamma^2 - 2\Gamma\cos(q_z d - \phi)} = \frac{2}{\beta J_\perp(q_\perp)} \tag{2.33}$$

in both limits. For $\gamma \to 0$, $\phi \to \alpha$ for all n. For $\beta\gamma \to \infty$, ϕ is a smooth function of temperature for $n > 2$, so the initial ordered phase is in general incommensurate. Hence, there is no Lifshitz point. For $n = 2$ on the other hand, $\phi = 0$, in which case the susceptibility diverges for $q_z d = 0$ and the initial ordered phase is ferromagnetic. In this case, there will be a Lifshitz point in the phase diagram.

These results give rise to the possibility of a sequence of commensurate phases for $n > 2$ as the temperature is reduced below the initial order-disorder transition temperature. While the above considerations support our conjecture concerning the nature of the initial order-disorder transition, the method used does not apply below the initial ordered phase. In order to determine qualitative nature of the phase diagram as the temperature is lowered below the transition to the initial ordered phase, we further investigate the mean-field model

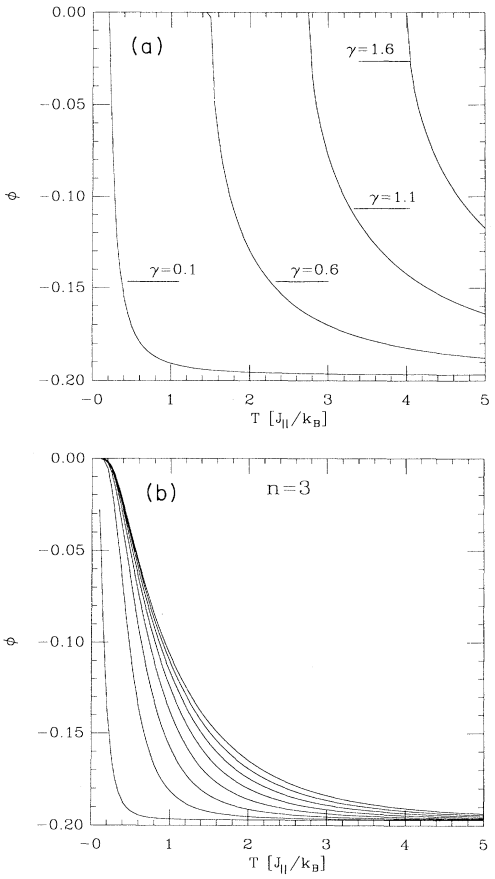

FIG. 2. The phase $\phi = \arg\lambda_{0,1}$ as a function of temperature for (a) $n = 2$ ($\gamma = 0.1$, 0.6, 1.1, and 1.6), and (b) $n = 3$ ($\gamma = 0.1, 0.6, 1.1, \ldots, 3.6$). In these cases, $J_\parallel = 1$ and $\alpha = 0.197$.

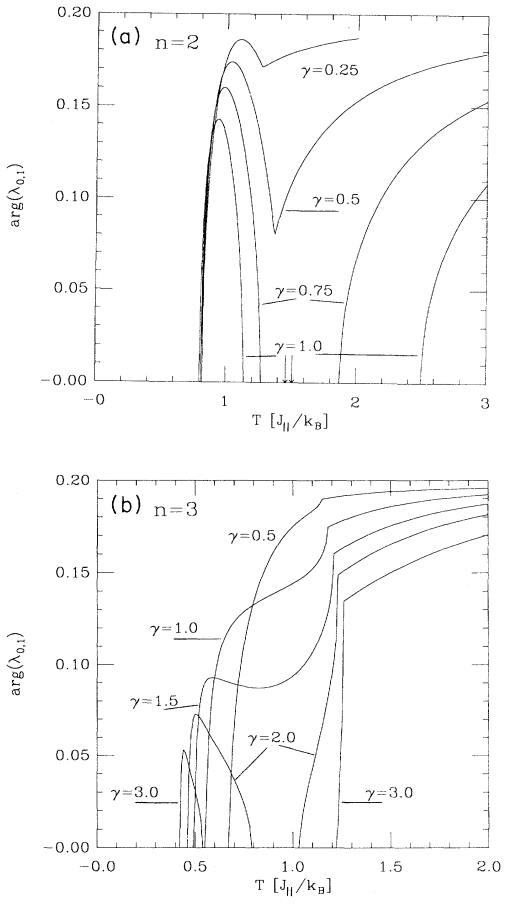

FIG. 3. Argument $\arg\lambda_{0,1}$ in the in-plane mean-field approximation for (a) $n = 2$ and (b) $n = 3$. In these graphs, $J_\parallel = zJ_\perp = 1$, and $\alpha = 0.197$. The critical temperatures for $n = 2$, $\gamma = 0.75$, and $\gamma = 1.0$ are indicated by the arrows. In these cases, the argument becomes zero at temperatures above T_c. Hence, the initial ordered phase is ferromagnetic.

$$H_{\rm mf} = -J_{\parallel}\sum_{ij}\cos(\theta_{i,j}-\theta_{i-1,j}-\alpha) - \frac{1}{2}J_{\perp}\sum_{\substack{i\\ \langle jj'\rangle}}[\cos\theta_{ij}\langle\cos\theta_{ij'}\rangle + \sin\theta_{ij}\langle\sin\theta_{ij'}\rangle] + \gamma\sum_{ij}\cos(n\theta_{ij}). \tag{2.34}$$

For ferromagnetic interchain coupling, $J_{\perp} > 0$, we make the ansatz

$$\langle\cos\theta_{i,j}\rangle = \langle\cos\theta_{i,j'}\rangle, \qquad \langle\sin\theta_{i,j}\rangle = \langle\sin\theta_{i,j'}\rangle, \tag{2.35}$$

that is, the indicated averages are independent of the chain index j. With this ansatz, together with $\mathbf{S}_{i,j}\cdot\langle\mathbf{S}_{i,j}\rangle = \mathbf{S}_{i,j'}\cdot\langle\mathbf{S}_{i,j'}\rangle$, we obtain an effective single-chain Hamiltonian

$$\tilde{H}_{\rm mf} = -J_{\parallel}\sum_{i}\cos(\theta_i-\theta_{i-1}-\alpha) + \gamma\sum_{i}\cos(n\theta_{i-1}) - zJ_{\perp}\sum_{i}\mathbf{S}_i\cdot\langle\mathbf{S}_i\rangle, \tag{2.36}$$

where z is the in-plane coordination number. This Hamiltonian can be studied by a transfer-integral formalism in which the equations

$$\int\frac{d\theta_i}{2\pi}e^{+\beta J_{\parallel}\cos(\theta_i-\theta_{i-1}-\alpha)-\beta\gamma\cos(n\theta_{i-1})+\beta J_{\perp}[\cos(\theta_i)\langle\cos\theta_i\rangle+\sin(\theta_i)\langle\sin\theta_i\rangle]}\Psi_k(\theta_i) = \lambda_k\Psi_k(\theta_{i-1}) \tag{2.37}$$

and

$$\langle S_i^{\mu}\rangle = \langle\Phi_0(\theta_i)\mid S_i^{\mu}\mid\Psi_0(\theta_i)\rangle \tag{2.38}$$

are solved self-consistently. The free energy per spin is then obtained as

$$F/N = -k_BT\ln\lambda_0 + \tfrac{1}{2}zJ_{\perp}\langle\mathbf{S}\rangle^2. \tag{2.39}$$

In Fig. 3, we show the phase $\phi = \arg\lambda_{0,1}$ of the intrachain correlation as a function of temperature for (a) $n = 2$ and (b) $n = 3$. For $n = 2$ and small values of γ ($\gamma = 0.25$ and $\gamma = 0.5$ in the figure), the initial disorder-order phase transition occurs at the downward cusps of the curves before the argument of the correlations has become zero. As γ increases, however, the phase of the correlations become zero at temperatures above the initial critical temperature, and the phase transition is paramagnetic to ferromagnetic. For $n = 3$, on the other hand, the phase transition occurs at the upward cusps of the curves, at which $\phi \neq 0$, into an initial incommensurate phase. This verifies the absence of a Lifshitz point for $n > 2$. For both $n = 2$ and $n = 3$, the initial incommensurate phases are followed by subsequent modulated phases. Note, however, that the calculations have not been performed with a high enough numerical precision to distinguish the individual modulated phases and their phase boundaries. As a consequence, the argument of the correlations appears to evolve continuously with temperature below the initial disorder-order transition. The nature of the phase diagrams in the $T-\gamma$ plane is depicted in Fig. 4. Note that both for $n = 2$ and $n = 3$, there is an interval of γ for which there is a reentrance to modulated phases as the temperature is decreased below an initial ferromagnetic phase, although the range of γ for which it occurs increases rapidly for increasing α. We will return to this in Sec. III. We have also performed Monte Carlo simulations to ensure that these conclusions are not due to artifacts in the mean-field approximation. In these simulations, we calculated the structure factor $S(0,0,q_z)$ as a function of temperature near the disorder-order transition. For twofold symmetry and γ sufficiently large, the structure factor developed a peak at $q_z = 0$ at the disorder-order transition. For small values of γ, as well as for threefold symmetry, the peak developed at a nonzero value of q_z. Hence, these simulations support our conclusions.

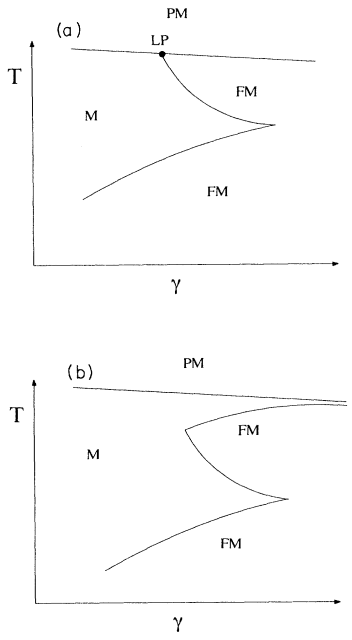

FIG. 4. Schematic high-temperature phase diagrams in the $T-\gamma$ plane for three-dimensional chiral molecules, and (a) $n = 2$ with the Lifshitz point marked by LP, and (b) $n > 2$. The high-temperature paramagnetic phase is denoted by PM, ordered modulated phases by M, and ferromagnetic phases by FM. The initial phase in the transition from paramagnetic to modulated phases at fixed γ is incommensurate.

B. Nonchiral models

We have found that for the chiral model, there is a fundamental difference between systems with twofold symmetry ($n = 2$), and systems with higher symmetry ($n > 2$) in that the phase diagram of the former possesses a Lifshitz point, while those of the latter do not. While there are real physical systems which have a preferred handedness, most systems do not. Therefore it is important to investigate if our main conclusion regarding the effect of the symmetry of the crystal lattice holds for nonchiral systems. In general, we do expect a qualitative difference between the two systems, since chiral and nonchiral systems belong to different universality classes.[23] However, these differences may be restricted only to finer details, such as critical exponents, and may not be discernible in the gross features of the phase diagrams. A complication for nonchiral systems is that the intrachain Hamiltonian must necessarily include both nearest-neighbor and next-nearest-neighbor interactions. We write the single-chain Hamiltonian as

$$H_0 = \sum_i \left[U(\theta_{i-2}) + V(\theta_{i-1},\theta_{i-2}) + W(\theta_i,\theta_{i-2})\right]. \tag{2.40}$$

Here, $U(\theta_{i-2})$ is the crystal-field term, $\gamma\cos(n\theta_{i-2})$, and $V(\theta_{i-1},\theta_{i-2})$ and $W(\theta_i,\theta_{i-2})$ are nearest- and next-nearest-neighbor interactions, respectively. We will assume that

$$\begin{aligned} V(\theta_{i-1},\theta_{i-2}) &= V(|\theta_{i-1}-\theta_{i-2}|), \\ W(\theta_i,\theta_{i-2}) &= W(|\theta_i-\theta_{i-2}|), \end{aligned} \tag{2.41}$$

where the difference in angles is only up to a modulus of π. One example of a nonchiral Hamiltonian is given by

$$\begin{aligned} V(\theta_{i-1},\theta_{i-2}) &= -J_1\mathbf{S}_{i-1}\cdot\mathbf{S}_{i-2}, \\ W(\theta_i,\theta_{i-2}) &= J_2\mathbf{S}_i\cdot\mathbf{S}_{i-2}, \end{aligned} \tag{2.42}$$

where $J_1, J_2 > 0$. The couplings J_1 and J_2 give rise to competing ferromagnetic and antiferromagnetic interactions along the chain axes, analogous to the ANNNI model.[2] This Hamiltonian has ground states which are helices with a pitch α given by $\cos\alpha = J_1/(4J_2)$, for $J_2/J_1 > 1/8$. Another example is given by

$$\begin{aligned} V(\theta_{i-1},\theta_{i-2}) &= \alpha_1\left(\theta_{i-1}-\theta_{i-2}\right)^2 + \alpha_2\left(\theta_i-\theta_{i-2}\right)^4, \\ W(\theta_i,\theta_{i-2}) &= -\gamma\left(\theta_i-2\theta_{i-1}+\theta_{i-2}\right)^2. \end{aligned} \tag{2.43}$$

This Hamiltonian can be obtained from Eq. (2.42) by a Taylor expansion, and has been used previously to study defect propagation in molecules of PTFE.[22]

As with the chiral models, we will study the nature of the intrachain correlations. Again, we first apply a transfer-integral formalism (see Appendix A) to the Hamiltonian H_0 with V and W given by Eqs. (2.42) or (2.43). The transfer-integral equation for the right eigenfunction is

$$\int_{-\pi}^{\pi}\frac{d\theta_i}{2\pi}e^{-\beta U(\theta_{i-2})-\beta V(\theta_{i-1},\theta_{i-2})-\beta W(\theta_i,\theta_{i-2})}\Psi_k(\theta_i,\theta_{i-1}) = \lambda_k\Psi_k(\theta_{i-1},\theta_{i-2}). \tag{2.44}$$

The corresponding equation for the left eigenfunction is

$$\int_{-\pi}^{\pi}\frac{d\theta_{i-1}}{2\pi}e^{-\beta U(\theta_{i-2})-\beta V(\theta_i,\theta_{i-1})-\beta W(\theta_{i+1},\theta_{i-1})}\Psi_k(\theta_{i-1}) = \lambda_k\Psi_k(\theta_{i+1},\theta_i). \tag{2.45}$$

We note that in spite of the fact that the Hamiltonian H_0 has degenerate ground states (left- and right-handed helices), the transfer-integral kernel is not symmetric. Hence, the left and right eigenfunctions are not equal, and the eigenvalues are in general complex (except for the largest eigenvalue λ_0).

Thermal averages and correlation functions are given by

$$\begin{aligned} \langle f(\theta_i)\rangle &= \int\frac{d\theta_i}{2\pi}\frac{d\theta_{i+1}}{2\pi}\Phi_0(\theta_{i+1},\theta_i)f(\theta_i)\Psi_0(\theta_{i+1},\theta_i) \\ &\equiv \langle 0\mid f(\theta_i)\mid 0\rangle, \end{aligned} \tag{2.46}$$

and

$$\langle f(\theta_i)g(\theta_j)\rangle = \sum_{k\neq 0}\langle 0\mid f(\theta_i)\mid k\rangle\langle k\mid g(\theta_j)\mid 0\rangle\left[\frac{\lambda_k}{\lambda_0}\right]^{-|i-j|}, \tag{2.47}$$

respectively.

The nature of the correlations are given by the second largest eigenvalue λ_1. If this eigenvalue is real and positive, the correlations are ferromagnetic. If on the other hand λ_1 is complex, these correlations are helical with a pitch given by $\phi = \arg\lambda_1$. In particular, we want to establish if nonchiral systems with a twofold crystal field do possess a Lifshitz point, while systems with higher symmetry do not. In the limit $\gamma \to 0$ the correlations are helical with a twist determined by V and W, and λ_1 is complex. Therefore, we need to establish the nature of the correlations in the limit $\gamma \to \infty$ to ascertain if a crossover to λ_1 really occurs. We can solve the transfer-integral equation exactly in the limit $\beta\gamma \to \infty$. For $n = 2$ we can in this limit map the Hamiltonian onto an Ising model by defining Ising spins σ_i by $\sigma_i = 1$ if $\theta_i = \frac{\pi}{2}$, and $\sigma_i = -1$ if $\theta_i = -\frac{\pi}{2}$. By using Eq. (2.41) and defining

$$\begin{aligned} a_1 &= e^{-\beta V(1,1)}, \quad a_2 = e^{-\beta V(1,-1)}, \\ b_1 &= e^{-\beta W(1,1)}, \quad b_2 = e^{-\beta W(1,-1)}, \end{aligned} \tag{2.48}$$

we obtain the following equation for the four largest eigenvalues:

$$\begin{vmatrix} \lambda_k - a_1b_1 & 0 & -a_1b_2 & 0 \\ -a_2b_2 & \lambda_k & -a_2b_1 & 0 \\ 0 & -a_2b_1 & \lambda_k & -a_2b_1 \\ 0 & -a_1b_2 & 0 & \lambda_k - a_1b_1 \end{vmatrix} = 0. \tag{2.49}$$

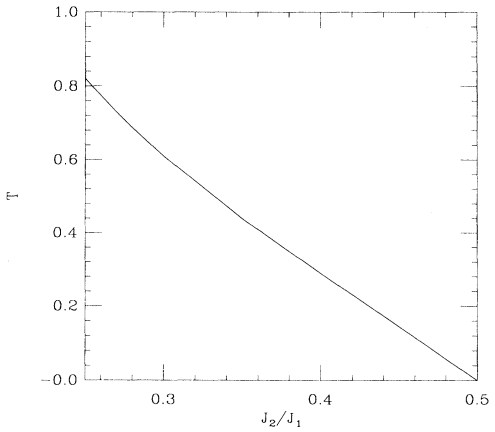

FIG. 5. In this plot is depicted the temperature given by $2\beta J_2 = \ln\cosh\beta J_1$ as a function of J_2/J_1 ($n = 2$). For the disorder-order transition to be from a paramagnetic to a ferromagnetic phase the interchain coupling must be so weak that the critical temperature falls below this graph.

We note that the determinant does not separate into a product of similar 2×2 determinants, which would ensure that the eigenvalues are all real. The equation can, however, be factored with the result

$$\left[\lambda_k^2 - (a_1 - a_2)b_1\lambda_k - a_1a_2(b_1^2 - b_2^2)\right]$$

$$\times \left[\lambda_k^2 - (a_1 + a_2)b_1\lambda_k + a_1a_2(b_1^2 - b_2^2)\right] = 0, \quad (2.50)$$

from which we find the eigenvalues

$$\lambda_0^{\pm} = \cosh\beta J_1 e^{-\beta J_2} \pm 2\left[\sinh^2 e^{-2\beta J_2} + e^{2\beta J_2}\right]^2, \quad (2.51)$$

$$\lambda_1^{\pm} = \sinh\beta J_1 e^{-\beta J_2} \pm 2\left[\cosh^2\beta J_1 e^{-2\beta J_2} - e^{2\beta J_2}\right]^{1/2}.$$

The two roots $\lambda_1^{\pm}$ are complex if $2\beta J_2 > \ln\cosh\beta J_1$. On the other hand, the chains have helical conformations only if $4J_2 > J_1$. In Fig. 5 is depicted the temperature given by $2\beta J_2 = \ln\cosh\beta J_1$ for $0.25 < J_2/J_1 < 0.5$. In order for the system to exhibit a paramagnetic-ferromagnetic phase transition, the critical temperature must fall below this line. The scale of the critical temperature is set by the interchain coupling. Hence, the paramagnetic-ferromagnetic transition can only occur for weak interchain interactions ($J_\perp$).

For $n > 2$, we can map the model in an analogous way onto an n-state model in the limit $\beta\gamma \to \infty$, leading to an $n \times n$ determinantal equation for the n largest eigenvalues. In general, the second largest eigenvalue is in these cases complex. We then conclude that systems with $n > 2$ do not have a crossover, so the initial ordered phase is (almost) always incommensurate, and there is no Lifshitz point.

We have also performed Monte Carlo simulations on the Hamiltonian H_0 with V and W given by Eq. (2.42). In these simulations, we calculated the structure factor $S(0, 0, q_z)$ at temperatures near an initial order-disorder transition. These simulations show that for γ large and $J_\perp \sim J_1$, $S(0, 0, q_z)$ develops a peak at a finite value of q_z at the temperature of the order-disorder transition, indicating that the initial ordered phase is modulated. For $n = 2$, γ large and $J_\perp \ll J_1$, which is the region in which we may expect a disordered-ferromagnetic transition, the simulations are inconclusive.

III. CONCLUSIONS AND DISCUSSION

We have in this paper investigated the effect of crystal-field strength and symmetry on the nature of the phase diagram of three-dimensional systems consisting of arrays of helical spin chains. The phase diagram of chiral chains in fields with twofold symmetry exhibits a Lifshitz point irrespectively of the preferred pitch which results from intrachain interactions alone. In contrast, the existence of a Lifshitz point in the phase diagram of nonchiral chains in arrays with twofold symmetry depends sensitively on the intrachain and interchain interactions. The phase diagrams of both chiral and nonchiral chains in arrays with higher symmetry than twofold do not exhibit a Lifshitz point. These results may have practical applications. The symmetry and strength of the crystal field may be affected by the application of external fields. Application of a uniaxial stress in the direction perpendicular to the chain axis in an array with, for example, hexagonal packing will lower the symmetry as the array deforms. As a result, if the chains initially are ordered helices with a nonzero pitch, their conformation may be altered to ferromagnetic as a result of the uniaxial stress. If the helices are optically active, this will dramatically alter their response to electromagnetic fields propagating in the direction along the chain axes. A transition of this kind from helices to zigzag chains is indeed observed in PTFE at high pressures (see Fig. 1). Our results here suggest that this transition could be universal. In addition, we have found that the phase diagrams (for the chiral molecules) exhibit reentrance to helical structures at temperatures *below* an initial ferromagnetic phase. This behavior, too, is observed in PTFE at high pressures, where there is a transition from the (ferromagnetic) phase III to the incommensurate low-temperature phase II as the temperature is lowered.

ACKNOWLEDGMENTS

It is a pleasure to acknowledge Phil Taylor's insightful help at the early stages of this work. We would also like to thank Scott McCullough and Martin Plumer for valuable comments on the manuscript.

[1]P. Bak and J. von Boehm, Phys. Rev. B **21**, 5297 (1980).
[2]A recent review of axial Ising models, including the ANNNI and the chiral clock model is given by J. Yeoman, Solid State Phys. **41**, 151 (1988).
[3]W. Selke, Phys. Rep. **170**, 213 (1988).
[4]W. S. McCullough, Phys. Rev. B **46**, 5084 (1992).
[5]R.A. Cowley and A.D. Bruce, J. Phys. C **11**, 3577 (1978).
[6]Note, however, that for the chiral clock model, the mean-field phase diagram at low temperatures does not agree with exact low-temperature expansions (see Ref. 3).
[7]G. Natta and P.J. Corradini, J. Polym. Sci. **39**, 29 (1959).
[8]Y. Saruyama, J. Chem. Phys. **78**, 2077 (1983).
[9]K. Matsushige *et al.,* Jpn. J. Appl. Phys. **5**, 681 (1977).
[10]R.G. Brown, J. Chem. Phys. **40**, 2900 (1964).
[11]E.S. Clark, J.J. Weeks, and R.K. Eby, Am. Chem. Soc. Symp. Ser. **141**, 183 (1980).
[12]For a recent review on chiral biomolecules, see V.A. Avetsikov, V.I. Goldaskii, and V.V. Kuz'imin, Phys. Today **44**, No. 7, 33 (1991).
[13]O. Vogl and G.D. Jaycox, Polymer **28**, 2179 (1987).
[14]O. Heinonen and P.L. Taylor, Polymer **32**, 2155 (1991).
[15]By "almost always," we shall mean everywhere in the phase diagram except for on a set of measure zero, where the intrachain interactions are compatible with the interchain interactions.
[16]H. Shiba, Prog. Theor. Phys. **64**, 466 (1980).
[17]See, for example, A.J. Hopfinger and P.L. Taylor, Acc. Chem. Res. **12**, 217 (1979).
[18]Note that while these methods have given excellent results for other three-dimensional systems with competing interactions, such as the stacked triangular antiferromagnetic Ising model (see Ref. 16), or the chiral clock model (see Ref. 4), they can fail completely in two dimensions.
[19]D.J. Scalapino, M. Sears, and R.A. Ferrell, Phys. Rev. B **6**, 3409 (1972).
[20]Note that it has been argued that the two-dimensional three-state chiral clock model has no Lifshitz point (see Ref. 3).
[21]D.J. Scalapino, Y. Imry, and P. Pincus, Phys. Rev. B **11**, 2042 (1975).
[22]O. Heinonen and P.L. Taylor, Polymer **30**, 585 (1989).
[23]H. Kawamura, Phys. Rev. B **38**, 4916 (1988).